



TITLE:

<Advanced Research Center for Beam Science>Electron Microscopy and Crystal Chemistry

AUTHOR(S):

CITATION:

<Advanced Research Center for Beam Science>Electron Microscopy and Crystal Chemistry. ICR Annual Report 2016, 23: 46-47

ISSUE DATE:

2016

URL:

<http://hdl.handle.net/2433/219047>

RIGHT:

Copyright © 2017 Institute for Chemical Research, Kyoto University

Advanced Research Center for Beam Science – Electron Microscopy and Crystal Chemistry –

<http://eels.kuicr.kyoto-u.ac.jp/Root/English>



Prof
KURATA, Hiroki
(D Sc)



Assist Prof
NEMOTO, Takashi
(D Sc)



Assist Prof
HARUTA, Mitsutaka
(D Sc)



Program-specific Res*
OGAWA, Tetsuya
(D Sc)



Program-specific Res*
KIYOMURA, Tsutomu

*Nanotechnology Platform

Students

FUJIYOSHI, Yoshifumi (D3)
YAMAGUCHI, Atsushi (D3)

LAI, Ming Wei (D2)
INOUE, Shota (M2)

HIGUCHI, Hiroki (M1)

Guest Scholar

SCHAPER, Andreas Karl (Ph D) Phillips University of Marburg, Germany, 26 September–17 October

Scope of Research

We study crystallographic and electronic structures of materials and their transformations through direct imaging of atoms or molecules by high-resolution electron spectromicroscopy, which realizes energy-filtered imaging and electron energy-loss spectroscopy as well as high-resolution imaging. By combining this with scanning probe microscopy, we cover the following subjects: 1) direct structure analysis, electron crystallographic analysis, 2) epitaxial growth of molecules, 3) structure formation in solutions, and 4) fabrication of low-dimensional functional assemblies.

KEYWORDS

EELS
STEM
Elemental Ratio
Surface Plasmon
Electronic Structure



Selected Publications

Haruta, M.; Kurata, H., Direct Observation of Crystal Defects in an Organic Molecular Crystals of Copper Hexachlorophthalocyanine by STEM-EELS, *Sci. Rep.*, **2**, [252-1]-[252-4] (2012).

Aso, R.; Kan, D.; Shimakawa, Y.; Kurata, H., Atomic Level Observation of Octahedral Distortions at the Perovskite Oxide Heterointerface, *Sci. Rep.*, **3**, [2214-1]-[2214-6] (2013).

Saito, H.; Namura, K.; Suzuki, M.; Kurata, H., Dispersion Relations for Coupled Surface Plasmon-polariton Modes Excited in Multilayer Structures, *Microscopy*, **63**, 85-93 (2014).

Saito, H.; Kurata, H., Formation of a Hybrid Plasmonic Waveguide Mode Probed by Dispersion Measurement, *J. Appl. Phys.*, **117**, [133107-1]-[133107-7] (2015).

Haruta, M.; Hosaka, Y.; Ichikawa, N.; Saito, T.; Shimakawa, Y.; Kurata, H., Determination of Elemental Ratio in an Atomic Column by Electron Energy-Loss Spectroscopy, *ACS Nano*, **10**, 6680-6684 (2016).

Determination of Elemental Ratio in an Atomic Column by Electron Energy Loss Spectroscopy

Elemental mapping with atomic-column resolution can be obtained using electron energy loss spectroscopy (EELS) combined with scanning transmission electron microscopy (STEM). One step in STEM-EELS is quantitative determination of elemental ratio in an atomic column. However, during elemental mapping using STEM-EELS, the elemental signals do not necessarily localize at atomic-column positions. The spatial resolution of an EELS signal is constrained by the delocalization of inelastic scattering. Careful attention to the mixing of signals from neighboring atomic-columns is required to analyze a spectrum at a single point. In the present study, the elemental ratio of Fe to Mn at octahedral and tetrahedral sites in brownmillerite $\text{Ca}_2\text{Fe}_{1.07}\text{Mn}_{0.93}\text{O}_5$ was determined quantitatively with atomic resolution using STEM-EELS. This study presents the experimental criteria for semiquantitative analysis of the $L_{2,3}$ -edges of Fe and Mn in a perovskite-related structure.

A HAADF image along the $[101]$ direction and an EELS data cube for the Fe and Mn $L_{2,3}$ -edges were simultaneously collected using an aberration-corrected JEM ARM-200F operating at 80 kV with a probe-forming aperture of 21.3 mrad. Spectra were recorded as line scans along the $\langle 010 \rangle$ direction. The scan step was 0.19 Å/pixel, which corresponded to 20 segment divisions in the B–B' cation distance. In the present research, the line-profiling method was used instead of two-dimensional mapping to avoid some practical problems (damage and stability) due to oversampling conditions.

Figure 1 shows a HAADF image with the projected structure overlaid. The cation $L_{2,3}$ -edge intensities after background-subtraction are shown in Figure 2b. The individual spectra extracted from the octahedral and tetrahedral sites contain a weak intensity from the nonpreferred cation at both polyhedral sites, as shown in Figure 2d. The delocalization factors of the Fe and Mn $L_{2,3}$ -edge excitations were approximately 1.2 and 1.3 Å, respectively, which are small enough to resolve the atomic distance (3.8 Å) between B and B' cations. The relative composition profiles obtained by quantifying the intensity at each spatial increment in the elemental profiles of Figure 2b are shown in Figure 2c. The relative composition profiles resembled wide isosceles trapezoids. The elemental profile reflects the one-dimensional distribution of excitation probabilities for a specific energy loss; a maximal excitation should occur just above each atomic position. In contrast, the relative composition profile should be constant near each atomic position if the spectra contain only the contribution from illuminated atomic columns. The flat region of the relative

composition profile (Figure 2c) indicates very little contribution from nearest neighbor columns and the quantitative analysis is achieved near-atomic resolution. Such a profile can be obtained only by oversampling of spectral data. The present experiment found that the relative composition profile was nearly constant within a 1.2 Å radius around the atomic position of each polyhedral site. The average ratio of Fe to Mn in this flat region (Figure 2c) was $(17.5:82.5) \pm 5.9$ in octahedral sites and $(81.6:18.4) \pm 6.0$ in tetrahedral sites. The result at octahedral sites roughly agreed with previous results from neutron diffraction, $(14.4:85.6) \pm 0.2$. Simple multislice calculations were used to estimate the error due to electron dechanneling combined with a delocalization factor. The Mn atomic fraction profile derived from EELS intensity ratio was calculated by assuming “true fractions” of Mn at octahedral site, $x=0.87$. The simulated profile accurately reproduced the flat region near an octahedral site, as expected, with a radius of 0.9 Å, which agreed well with the experimental value. For a thin sample ($t < 10$ nm), the estimated error was negligibly small.

Results showed that relative composition profiles with an isosceles trapezoid-shape are useful for quantifying the resolution of measurements. An area with a radius of about 1.2 Å surrounded both atomic sites and provided information at near-atomic resolution. This study demonstrates that the experimental spectra at the $L_{2,3}$ -edge, obtained from octahedral atomic columns of 3d transition metals in perovskite-like structures, can be quantitatively interpreted with an uncertainty of 10% (accuracy of calculated partial cross sections of L-shell using Hartree-Slater model) without full quantum mechanical simulation.

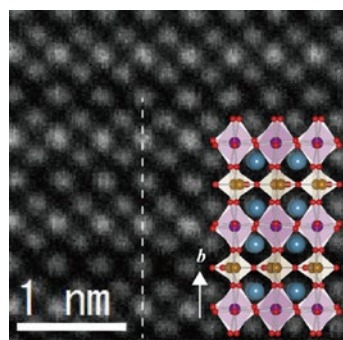


Figure 1. HAADF image of the $[101]$ direction in $\text{Ca}_2\text{Fe}_{1.07}\text{Mn}_{0.93}\text{O}_5$. Inset shows the corresponding structure. Spectral imaging was performed along the dashed line.

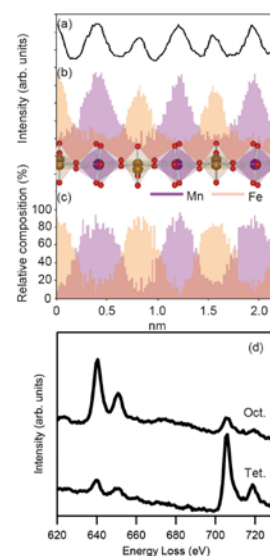


Figure 2. Line profiles and spectra for $\text{Ca}_2\text{Fe}_{1.07}\text{Mn}_{0.93}\text{O}_5$: (a) HAADF profiles; (b) EELS elemental $\langle 010 \rangle$ line profiles for the $L_{2,3}$ -edges of Fe and Mn; (c) profile of the relative compositions of Fe and Mn; (d) spectra measured above the octahedral and tetrahedral cations.